AGU PUBLICATIONS

Tectonics

RESEARCH ARTICLE
10.1002/2015TC003976

Key Points:
- AMS results are consistent with the outcrop features, the compaction, and paleomagnetic results
- The deformation along the southwest Gondwana boundary propagated toward the foreland during Permian
- The direction of the shortening indicates that the maximum effort became from the southwest

Correspondence to:
G. Arzadún,
guadalupe.arzadun@gmail.com

Citation:
Arzadún, G., R. N. Tomezzoli, and N. N. Cesaretti (2016), Tectonic insight based on anisotropy of magnetic susceptibility and compaction studies in the Sierras Australes thrust and fold belt (southwest Gondwana boundary, Argentina), *Tectonics*, *35*, doi:10.1002/2015TC003976.

Received 17 JUL 2015
Accepted 16 MAR 2016
Accepted article online 28 MAR 2016

Tectonic insight based on anisotropy of magnetic susceptibility and compaction studies in the Sierras Australes thrust and fold belt (southwest Gondwana boundary, Argentina)

Guadalupe Arzadún[1,2], Renata N. Tomezzoli[2,3], and Nora N. Cesaretti[1]

[1]Departamento de Geología, Universidad Nacional del Sur, Bahía Blanca, Argentina, [2]CONICET—Consejo Nacional de Investigaciones Científicas y Técnicas, Buenos Aires, Argentina, [3]Departamento de Geología, Universidad de Buenos Aires, IGEBA, Buenos Aires, Argentina

Abstract The Sierras Australes fold and thrust belt (Buenos Aires Province, Argentina) was in the southwestern Gondwanaland margin during the Paleozoic. The Tunas Formation (Permian) is exposed along the eastern part of it and continues eastward beneath the Claromecó Basin. Anisotropy of magnetic susceptibility (AMS) and compaction studies are described and compared with previous paleomagnetic studies with the aim of determining direction and magnitude of the main stresses acting during the sedimentation of the Tunas Formation. The anisotropy ellipsoids are triaxial with oblate or prolate shapes, reflecting different stages of layer parallel shortening during the evolution of the basin. K_{max} axes trend NW-SE, parallel to the fold axes, while K_{min} move from a horizontal (base) to a vertical orientation at the top of the succession, showing a change from a tectonic to almost a sedimentary fabric. The magnitude of anisotropy and compaction degree decreases toward the top of the succession. The AMS results are consistent with the outcrop structural observations and the compaction and paleomagnetic data. Regional pattern indicates a compression from the SW along this part of Gondwana, with a migration of the orogenic front and attenuation toward the NE in the foreland basin during the Upper Paleozoic. This deformation, locally assigned to the San Rafael noncollisional orogenic phase, is the result of the latitudinal movements toward the Equator of Gondwana (southern plates) and Laurentia (northern plates) during the Permian. This movement is the result of a rearrangement of the microplates that collided with Gondwana during the Late Devonian, to configure Pangea during the Triassic.

1. Introduction

In the Sierras Australes of Buenos Aires Province, sited between 37°–39° south latitude and 61°–63° west longitude, a portion of the Claromecó Basin is exposed [*Ramos*, 1984; *Kostadinoff and Prozzi*, 1998; *Lesta and Sylwan*, 2005; *Pángaro and Ramos*, 2012] (Figure 1a). The Sierras Australes sedimentary rocks were deposited in a basin developed along the southwestern margin of the Gondwana supercontinent during the Paleozoic [*Keidel*, 1916; *Harrington*, 1947; *Suero*, 1972; *Kilmurray*, 1975; *Ramos*, 1984; *Von Gosen et al.*, 1990], and it is assumed that they were part of a large system of basins, which includes the rocks of the Cape Fold Belt of South Africa [*Du Toit*, 1927; *Zambrano*, 1974]. They are interpreted as part of the Hesperides Basin during the Pennsylvanian to the Early Triassic, which is in lateral continuity with the Kalahari, Karoo and Chaco-Paraná basins in Africa and South America, comprising a depocenter of over 3,000,000 km^2 [*Pángaro et al.*, 2015].

The Sierras Australes are a fold and thrust belt with a northeast vergence in present geographical coordinates [*Von Gosen et al.*, 1991; *Tomezzoli and Cristallini*, 1998, 2004]. The outcrops are composed of rocks from Late Precambrian in the west, to Permian successions in the east, unconformable overlain by Cenozoic deposits (Figure 1b). These rocks are subdivided into three main orographic units: Curamalal, Ventana, and Pillahuincó groups that have an important difference in the grade of metamorphism and in the style of the deformation [*Harrington*, 1947] (Figure 1). In the Curamalal and Ventana Groups, situated in the western sector, there is a lower greenschist metamorphism [*Cobbold et al.*, 1987; *Buggisch*, 1987], while in the Pillahuincó Group, situated in the eastern sector, there is a diagenesis range [*Iñiguez and Andreis*, 1971; *Buggisch*, 1987; *Von Gosen et al.*, 1989]. The western sector presents more deformed strata in the Sierras de Curamalal, Bravard, and Ventana, while in the eastern sector, in the Sierras de las Tunas and Pillahuincó, there is a characteristically more open folding (Figure 2).

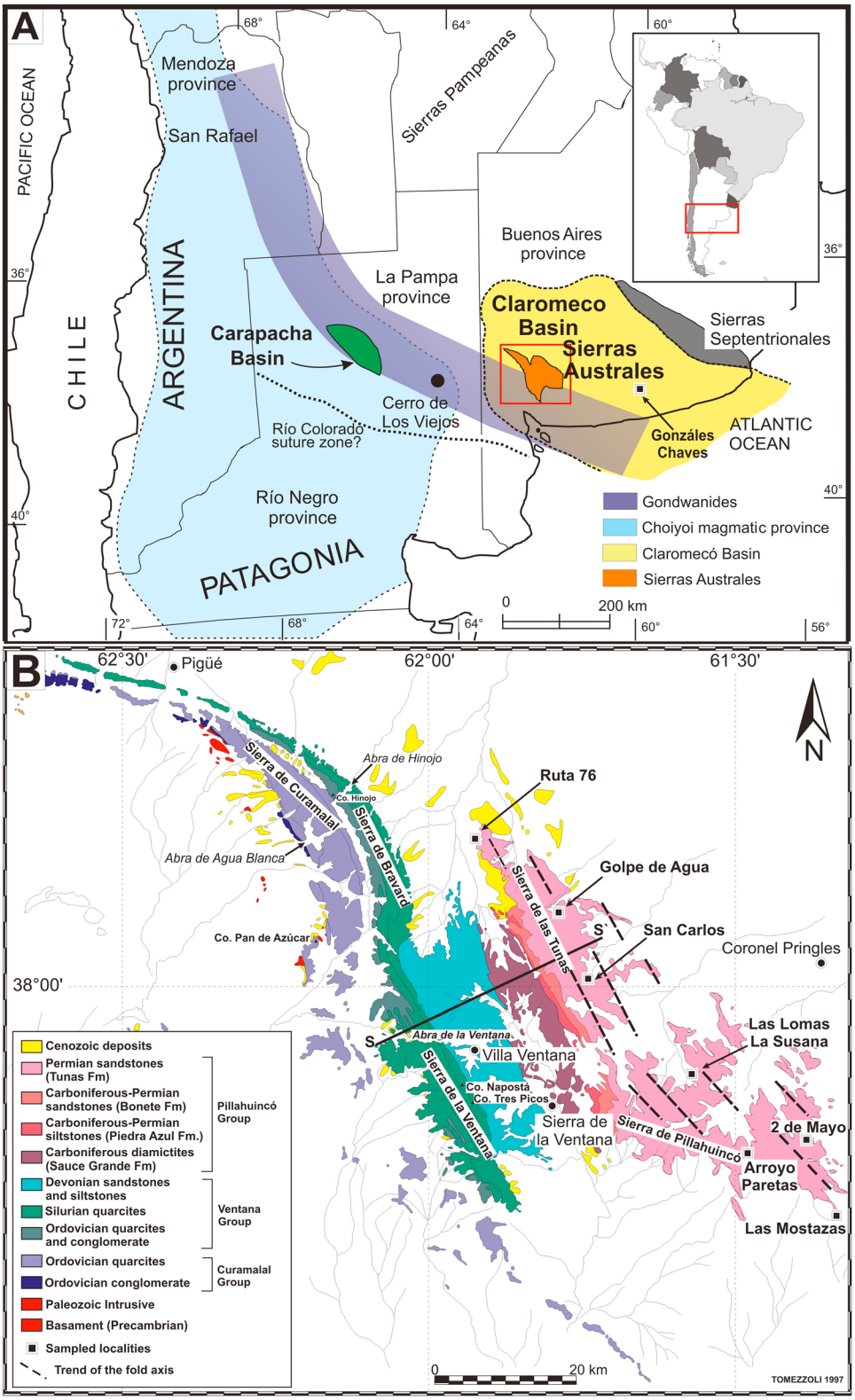

Figure 1. (a) Location of the Sierras Australes thrust and fold belt (orange) in the southwest of Buenos Aires Province, Argentina, and other surrounding geological provinces (Carapacha Basin in green and Choiyoi magmatic Province in light blue). The study area is the exposed portion of the Claromecó Basin (in yellow) developed in the southwestern margin of the Gondwanides belt (in violet). (b) Geologic map of the Sierras Australes to the southwest of Buenos Aires Province, Argentina, modified from *Suero* [1972]. Location of the eight sampled localities of the Tunas Formation exposed on the eastern side of the Sierras Australes. The fold axes trend northwest-southeast. S-S` is the localization of a structural section (Figure 2).

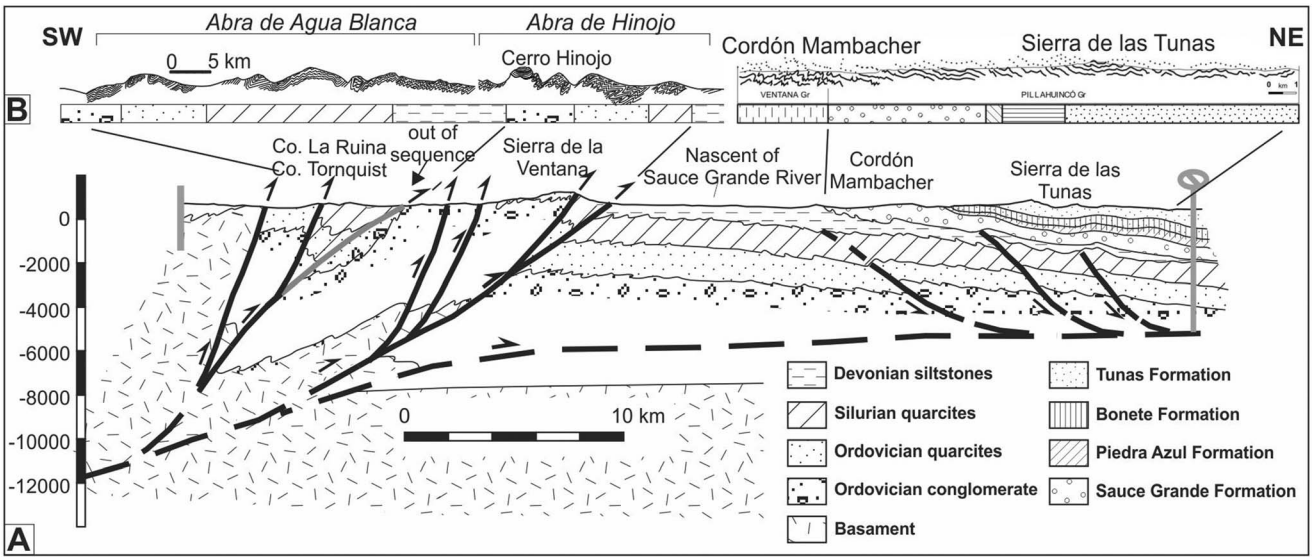

Figure 2. Structural cross section of the Sierras Australes: (a) general and (b) detailed (taken from *Tomezzoli and Cristallini* [2004]). Notice that the western sector presents more deformed strata than the eastern sector, see shortening values.

The outcrops of the Sierras Australes continue in the subsurface to the east, with some small isolated outcrops near the locality of Gonzáles Cháves were the beds are horizontal [*Monteverde*, 1937; *Amos and Urien*, 1968; *Zambrano*, 1974; *Llambías and Prozzi*, 1975; *Kostadinoff and Font de Affolter*, 1982; *Lesta and Sylwan*, 2005].

The structure of the Sierras Australes was initially interpreted as a system deformed dominantly by folding [*Harrington*, 1947]. *Ramos* [1984], *Chernicoff et al*. [2013], and *Ramos et al*. [2013] assumed that the Sierras Australes structure is the product of an intercontinental collision between Patagonia and Gondwana. Other authors suggest a system of continental blocks which move as a result of a tectonic event producing crustal fragmentation through transformed faults [*Kostadinoff*, 1993; *Álvarez*, 2004; *Kostadinoff*, 2007; *Gregori et al*., 2003, 2008]. *Tomezzoli* [2012] suggests that the deformation in the area might be a combination of these processes. Some contributions analyzed the structures at different length scales and its evolution has been interpreted through various tectonic models. *Rossello and Massabie* [1981] suggested a coaxial deformation model and interpreted the structures as the result of a nonrotational pure shear deformation. Other authors assumed a noncoaxial deformation model, with conditions of deformation dominated by simple shear [*Cobbold et al*., 1987, 1991; *Japas*, 1995a, 1995b, 1999; *Rossello and Massabie*, 1992; *von Gosen et al*., 1990].

Based on paleomagnetic results [*Tomezzoli and Vilas*, 1999], on recrystallization age of illite [*Buggisch*, 1987] and the presence of growth strata [*López Gamundi et al*., 1995], the age of the deformation of the Sierras Australes has been assigned to the Permian, despite some authors assuming that it began during the Devonian-Carboniferous [*Tomezzoli*, 2012].

The aim of this paper is to characterize the deformation associated with the southeast margin of the Gondwana supercontinent by determining the direction and magnitude of the main shortening that affected the Permian units of the Sierras Australes. These results will be correlated with previously obtained paleomagnetic and stratigraphic determinations [*Tomezzoli and Vilas*, 1999; *Tomezzoli*, 2001], with compaction data, and with anisotropy of magnetic susceptibility (AMS) data of nearby basins belonging to Gondwana during the Permian.

2. Methodology

The anisotropy of magnetic susceptibility (AMS) is an effective technique that can be used as a proxy to the petrofabric of the rock. The method allows the measurement of the composite susceptibility fabric of all the phases present in the rock [*Graham*, 1954; *Borradaile*, 1988; *Jackson*, 1991; *Tarling and Hrouda*, 1993]. The AMS measurement was carried out with a Kappabridge MKF-1a magnetometer at the Laboratorio de Paleomagnetismo "Daniel A. Valencio," Departamento de Geología, Universidad de Buenos Aires.

Table 1. Outcrop Data in Each Locality of the Tunas Formation[a]

Locality	Location	Site	Facies	N	B. plane	F	$F_{average}$	L	$L_{average}$
Ruta 76	Sierra de las Tunas	1	1	13	323/35°	1.009	1.0087	1.018	1.0107
			2	3					
		2	1	2		1.008		1.009	
			2	4					
		3	1	3					
			2	6		1.009		1.005	
Ea. Golpe de Agua	Sierra de las Tunas	1	1	9	323/34°	1.019	1.0164	1.038	1.0209
		2	1	11	325/35°	1.01		1.01	
		3	1	7	048/04°	1.019		1.041	
		4	1	5	137/32°	1.015		1.012	
		5	1	7	303/22°	1.018		1.032	
		6	2	6	134/36°	1.004		1.008	
		7	2	7	137/24°	1.042		1.018	
		8	2	10	320/45°	1.004		1.008	
Ea. San Carlos	Sierra de las Tunas	1	1	7	312/24°	1.011	1.0117	1.077	1.0251
		2	1	13	151/22°	1.014		1.017	
		3	1	18	132/09°	1.014		1.019	
		4	1	12	115/30°	1.013		1.027	
		5	1	11	095/12°	1.015		1.013	
		6	1	14	330/31°	1.013		1.006	
		7	1	14	116/26°	1.018		1.046	
		8	1	10	078/12°	1.008		1.013	
		9	1	11	329/18°	1.004		1.004	
		10	1	15	130/18°	1.006		1.033	
		11	1	6	123/13°	1.018		1.037	
		12	1	16	094/19°	1.006		1.009	
Ea. La Susana	Sierra de Pillahuincó	1	1	6	135/27°	1.028	1.0116	1.002	1.0080
		2	1	7	349/31°	1.014		1.012	
		3	1	3	312/29°	1.014		1.014	
			3	3					
		4	2	11	135/27°	1.008		1.004	
		5	1	10	150/18°	1.007		1.009	
		6	1	6	158/19°	1.006		1.007	
		7	2	10	158/19°	1.004		1.008	
A° Paretas	Sierra de Pillahuincó	1	1	7	135/23°	1.007	1.0097	1.018	1.0323
		2	1	10	148 /28°	1.009		1.032	
		3	1	11	155 /30°	1.013		1.047	
Las Mostazas	Sierra de Pillahuincó	1	1	2	240/07°	1.019	1.0193	1.04	1.0211
		2	1	15	118/29°	1.02		1.019	
		3	1	11	148/05°	1.028		1.027	
		4	1	8	134/12°	1.018		1.016	
		5	1	14	138/09°	1.017		1.016	
		6	1	5	154/10°	1.014		1.012	
		7	1	1	240/07°	1.019		1.018	
Ea. 2 de Mayo	Sierra de Pillahuincó	1	2	12	135/27°	1.004	1.0083	1.009	1.0148
		2	2	20	313/37°	1.005		1.013	
		3	2	20	318/30°	1.009		1.018	
		4	3	23	311/33°	1.015		1.019	
Gonzáles Chaves	Claromecó Basin	1	1	1	Horizontal	1.006	1.0070	1.006	1.0190
		3	1	10	Horizontal	1.008		1.032	

[a] N: Number of specimens per site. B. Plane: bedding strike (0°–360°) and dip (90° clockwise, from given strike, 0°–90°). $F = K_{int}/K_{min}$: Foliation [*Flinn*, 1962]. $L = K_{max}/K_{int}$: Lineation.

A total of 432 previously sampled specimens for paleomagnetic studies were measured [*Tomezzoli*, 1997]. They come from eight localities occupying different stratigraphic positions of the Tunas Formation. Samples were collected from: three localities at the base, along the Sierra de las Tunas: Ruta 76, San Carlos and Golpe de Agua; four localities at the Sierra de Pillahuincó: La Susana, 2 de Mayo, Arroyo Paretas and Las Mostazas (Figure 1a and Table 1); and one locality in the Claromecó Basin at the Gonzáles Chaves locality (Figure 1b and Table 1). At least four hand samples or six drill cores were collected at each of the 47 sites. They were orientated

in the field using magnetic and/or sun compasses. Usually, three standard cylindrical specimens (2.2 cm long × 2.5 cm diameter) were cut from each core (Table 1).

The samples belong to three sedimentary facies, distinguished using the field criteria proposed by *Walker and James* [1992]. The petrography and compaction degree of the different sedimentary facies were determined using a petrographic microscope on thin polished sections. The compaction degree was determinate by the *tight packing index* (TPI) [*Wilson and McBride*, 1988], defined as the sum of straight (*r*), concave convex (*c*), and sutured (*s*) contacts between grains of sandstone, divided by the total number of contacts (T_c):

$$\mathrm{TPI} = (r + c + s)/T_c.$$

The different types of contacts were identified using the criteria proposed by *Taylor* [1950]: floating, punctual, straight, concave convex, and sutured. The count of the different types of contacts between the grains was made in eleven (11) samples from five (5) localities: Ruta 76 (Sierra de las Tunas), La Susana, 2 de Mayo, Las Mostazas (Sierra de Pillahuincó), and Gonzáles Chaves (Claromecó Basin). The JMicroVision program was used as a point counter, whereby 300–500 points in each sample were counted [*Arzadún*, 2015]. This way, the TPI was calculated in the samples that belong to Facies 2, because their medium grain size allows for easy identification of the contacts between grains.

To corroborate the presence of hematite, an X-ray analysis was carried out with a Rigaku Denki Geigerflex Max III C equipment, with graphite monochromator, Kα of Cu radiation and scan rate of 2° per minute.

3. Geological Setting

In this work, the sampling was restricted to the Tunas Formation [*Harrington*, 1947], which is widely exposed on the eastern sector of the Sierras Australes, at the Sierra de las Tunas and at the Sierra de Pillahuincó and continues eastward beneath the Claromecó Basin, with some isolated outcrops in Gonzáles Chaves (Figure 1). This formation is the youngest unit of the Carboniferous-Permian Pillahuincó Group [*Harrington*, 1947], which is composed of the Sauce Grande, Piedra Azul, Bonete, and Tunas Formations (Figure 1b). The Tunas Formation is differentiated from the others on the basis of its mineral composition, a well-defined northeastward paleocurrent pattern, different depositional conditions, and the presence of growth folds [*López Gamundi et al*., 1995]. It comprises over 1200 m of yellow and grey fine-grained to medium-grained sandstones, green fine-grained sandstones with *Glossopteris* fossil leaves and red siltstones and claystones, with some interbedded tuff levels. These rocks were interpreted as part of a deltaic complex prograding toward the northeast [*Harrington*, 1947; *Iñiguez et al*., 1988; *Andreis et al*., 1989; *Andreis and Cladera*, 1992; *López Gamundi et al*., 1995; *Zavala et al*., 1993]. It is important to highlight the great contents of hematite in the rocks of the Tunas Formation [*Andreis et al*., 1979], which carries its syntectonic characteristic remanent magnetization [*Tomezzoli and Vilas*, 1999; *Tomezzoli*, 2001; *Arzadún*, 2015]. According to *Andreis et al*. [1989] it is likely that hematite had a primary origin, because its abundance correlates with the lithology (hematite is more abundant in the limestones).

The paleoflora associations of the Tunas Formation [*Archangelsky and Cúneo*, 1984] and its zircon datings in tuff of Arroyo Paretas locality, by sensitive high-resolution ion microprobe methodology, indicate an age of 280.8 ± 1.9 Ma (Early Permian) for these rocks [*López Gamundi et al*., 2013]. The structure of the Tunas Formation is characterized by cylindrical folds with horizontal axes and short wavelengths of some meters with no vergence, very different to the structure of the Curamalal and Ventana groups, which have a clear vergence toward the northeast (Figure 2). There are also differences inside the Tunas Formation structure itself. Toward its base the folds have well-defined limbs and the strata are dipping between 30° and 40° to the northeast or southwest; whereas to the top of the unit the folds tend to enlarge, their interlimb angles are bigger than in folds at the base and the strata are almost horizontal (Table 1).

Three different sedimentary facies of the Tunas Formation were sampled (Table 1) and they are described macroscopically and microscopically as follows:

1. Facies 1: consists of tabular beds with sharp bases of green fine-grained to very fine-grained sandstones, with parallel and ripple-cross lamination. It contains nodules and concretions of hematite, with ellipsoidal shape to the base and rounded shape to the top of the succession (Figures 3a and 3b). Microscopically, these sandstones are composed of clast of quartz, plagioclase, potassic feldspar, lithic fragments, and

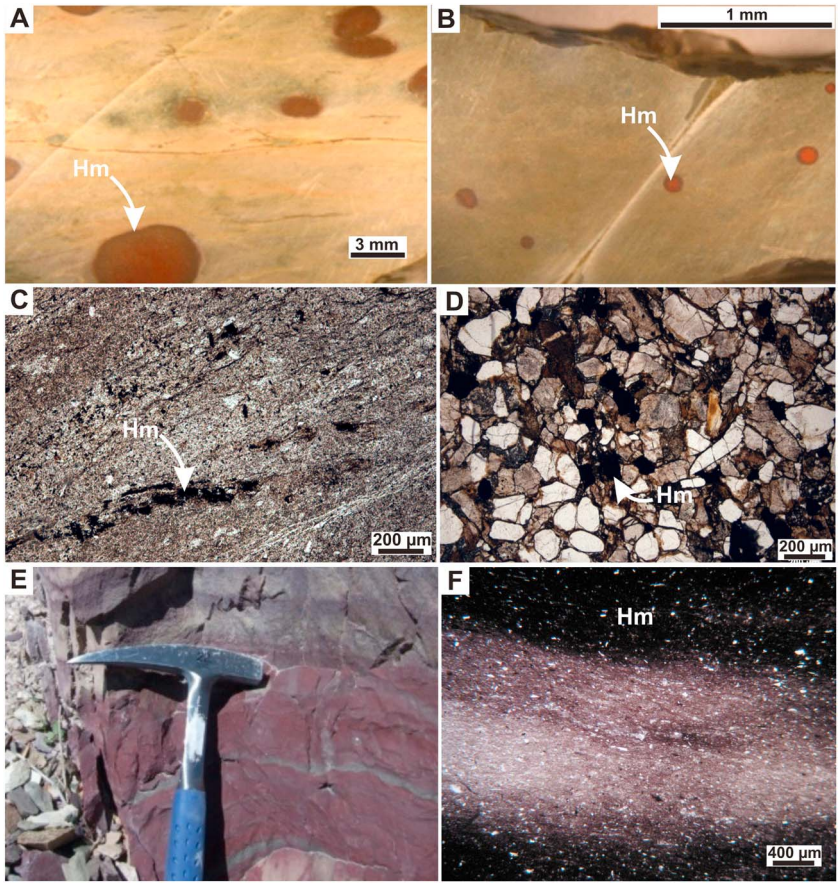

Figure 3. Different occurrences of hematite indistinctively exposed along the whole stratigraphic succession. Facies 1: (a) nodules with ellipsoid or rounded shapes in localities at the base of the Tunas Formation (west), (b) nodules with rounded shapes in localities to the top, and (c) intergranular cement (in thin section with parallel light). (d) Facies 2. Microscopic view (parallel light): hematite as detrital grains and as intergranular cement. Facies 3: red massive siltstones and claystones. (e) In outcrop. (f) Microscopic view (parallel light): hematite as intergranular cement.

minor mica (principally muscovite) and opaque minerals that consist of hematite. The matrix is formed by sericite and minor quartz and epidote and it has hematite cement (Figure 3c).

2. Facies 2: consists of lenticular beds with erosional bases of yellow medium-grained sandstones, with cross bedding. Microscopically, these sandstones are composed of clasts of quartz, plagioclase, potassic feldspar, lithic fragments of metamorphic and volcanic rocks, muscovite, and opaque minerals which consist in hematite. The matrix is formed by sericite, quartz, and epidote and it has cement composed of hematite and minor calcite in a few samples (Figure 3d).
3. Facies 3: consists of tabular massive beds with sharp bases of red siltstones and claystones (Figure 3e). Microscopically, this facies is composed of quartz, feldspar, and micas (muscovite, sericite, and chlorite) (Figure 3f).

The three facies are indistinctively exposed along the whole of the stratigraphic succession, from the base to the top.

4. Magnetic Mineralogy

The magnetic mineralogy is composed of diamagnetic, paramagnetic, and ferromagnetic minerals. Microscopically, some diamagnetic minerals were identified as quartz and calcite, other paramagnetic minerals as phyllosilicates (muscovite, sericite, and chlorite) and hematite as ferromagnetic mineral (Figures 3c, 3d, and 3f).

The presence of hematite in diverse facies was corroborated by X-ray analyses, by identifying its characteristic peaks at 33.15 and 19.83 (two-theta value) in the diffraction X-ray spectrum (Figure 4).

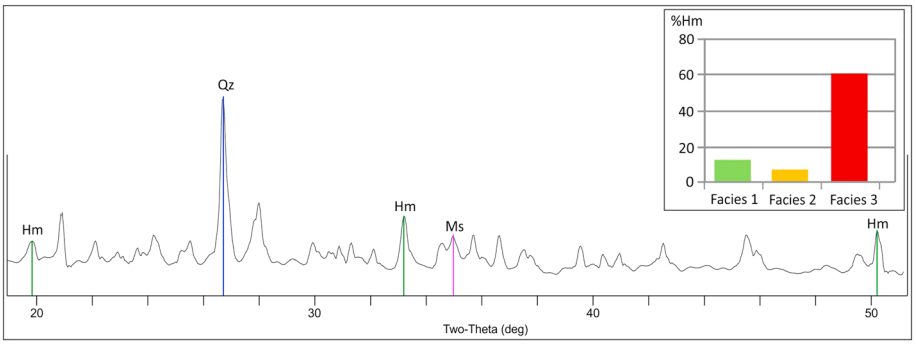

Figure 4. X-ray diffraction analysis showing the characteristic peaks of hematite (Hm) and the maximum peaks of other minerals: quartz (Qz) and muscovite (Ms). The inset shows the hematite percent content of each facies. The three facies can be found either at the base or at the top of the succession. The isolated paleomagnetic directions and the AMS patterns correlate more specifically to the stratigraphic position in the succession rather than the identified facies.

Hematite shows various forms of occurrences in the different facies with variable percentages: Facies 1 contains 15% of hematite as nodules and concretions, cement and as detrital grains (Figures 3a, 3b, 3c, and 4); Facies 2 contains 11% of hematite as detrital grains or as cement to a lesser extent (Figures 3d and 4); Facies 3 contains 60% of hematite as intergranular cement (Figures 3f and 4).

Hematite has a detrital and diagenetic origin: it is associated to the lithology as it has different shapes in the different facies and could have precipitated during an early diagenesis under oxidizing conditions [*Andreis et al*., 1989]. The nodules and concretions of hematite in the Tunas Formation were generated in situ and the cement could be generated by the same process of precipitation, and the detrital grains were transported and deposited by paleocurrents. The precipitation of hematite was favored in the finest grain size facies [*Arzadún et al*., 2014]. According to *Arzadún et al*. [2014], Facies 1 of the Tunas Formation can be interpreted as a waterbody similar to a lake with oxygenating characteristics; similar iron-rich nodules have been observed in lacustrine environments and have been interpreted as formed during early diagenesis in different localities around the world [*Yoshida et al*., 2006; *Bowen et al*., 2008].

More than 800 samples from the Tunas Formation were utilized in a previous paleomagnetic study, some of them utilized in this AMS study [*Tomezzoli*, 1997]. The prevalence of samples belonging to Facies 1 in some localities responds simply to the fact that it can be more easily sampled. All samples analyzed have hematite as nodules and concretions, cement and detrital grains.

The natural remanent magnetization intensities range between 0.5 and 90 mA m^{-1}. All samples exhibit similar behavior during progressive thermal demagnetization. Many of them were stable during experimental heating, with high coercitivity and unblocking temperatures from 630° to 680°C. These values strongly suggest that the magnetization is carried by hematite. The demagnetization by alternating field is not effective due to the high coercivity of hematite [*Tomezzoli*, 2001]. The average susceptibility measured is less than 5×10^{-5} SI (Table 2); these low values of K_{mean} are mainly consistent with contribution from the primary

Table 2. Average Parameters of the Anisotropy of Magnetic Susceptibility (AMS)[a]

Locality	Location	$K_{m\text{-average}}$	SD K_m	$P_{j\text{-average}}$	SD P_j	$T_{average}$	SD T
Ruta 76	Sierra de las Tunas	$1.75 \times e^{-04}$	$1.74 \times e^{-05}$	1.022	0.005	0.241	0.153
Ea. Golpe de Agua	Sierra de las Tunas	$1.55 \times e^{-04}$	$5.84 \times e^{-05}$	1.037	0.009	0.202	0.48
Ea. San Carlos	Sierra de las Tunas	$1.81 \times e^{-04}$	$2.30 \times e^{-05}$	1.035	0.009	0.209	0.262
Ea. La Susana	Sierra de Pillahuincó	$1.95 \times e^{-04}$	$4.51 \times e^{-05}$	1.019	0.01	0.000	0.309
A° Paretas	Sierra de Pillahuincó	$4.21 \times e^{-04}$	$5.12 \times e^{-05}$	1.047	0.024	−0.533	0.366
Las Mostazas	Sierra de Pillahuincó	$2.19 \times e^{-04}$	$6.87 \times e^{-05}$	1.039	0.025	−0.047	0.35
Ea. 2 de Mayo	Sierra de Pillahuincó	$1.91 \times e^{-04}$	$3.80 \times e^{-05}$	1.025	0.014	−0.289	0.172
Gonzáles Chaves	Claromecó Basin	$8.94 \times e^{-05}$	$1.61 \times e^{-04}$	1.017	0.021	0.126	0.254

[a] $K_m = K_{mean} = (K_{max} + K_{int} + K_{min})/3$: bulk volume susceptibility in SI units. $P_j = (K_{max}/K_{min})$: Degree of anisotropy [*Nagata*, 1961]. T: Jelinek's shape parameter [*Jelinek*, 1981] (lnF − nL)/(lnF + nL). SD: Standard deviation of each parameter.

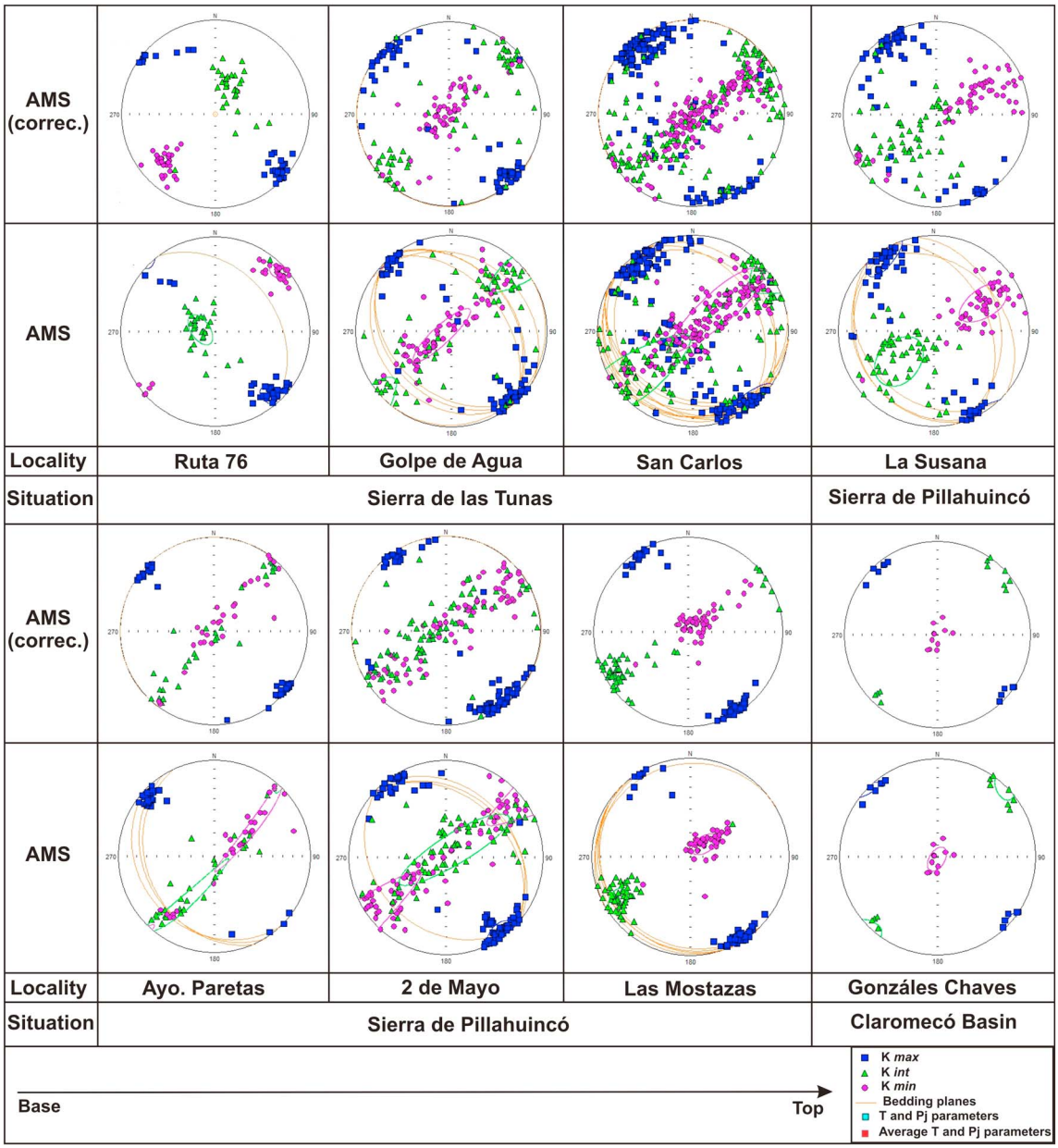

Figure 5. AMS results of the Tunas Formation along the different localities. From the base to the top of the stratigraphic column, the position of the K_{min} axes gradually changes, as well as the geometry of the structure. K_{max} remains NW-SE, while K_{min} migrates from a horizontal to a vertical position at the top of the sedimentary succession. Structure correction of AMS ellipsoids made by restoring the beds to the horizontal plane by a single rotation about strike. The data are in geographic coordinates with the respective bedding planes.

origin of hematite. However, the contribution of paramagnetic minerals such as phyllosilicates cannot be disregarded [*Tarling and Hrouda*, 1993].

5. AMS Results

In the Tunas Formation the AMS ellipsoids shape shows composite fabrics with good internal consistency among the data in every studied site. This enables the correlation between the structural features of each site with the AMS patterns, which depends on the stratigraphic position.

The K_{max} axes trend northwest-southeast, parallel to the fold axes (Figure 5). The K_{min} axis shows a bimodal distribution. At the base of the sedimentary column, on the westernmost and also highly deformed

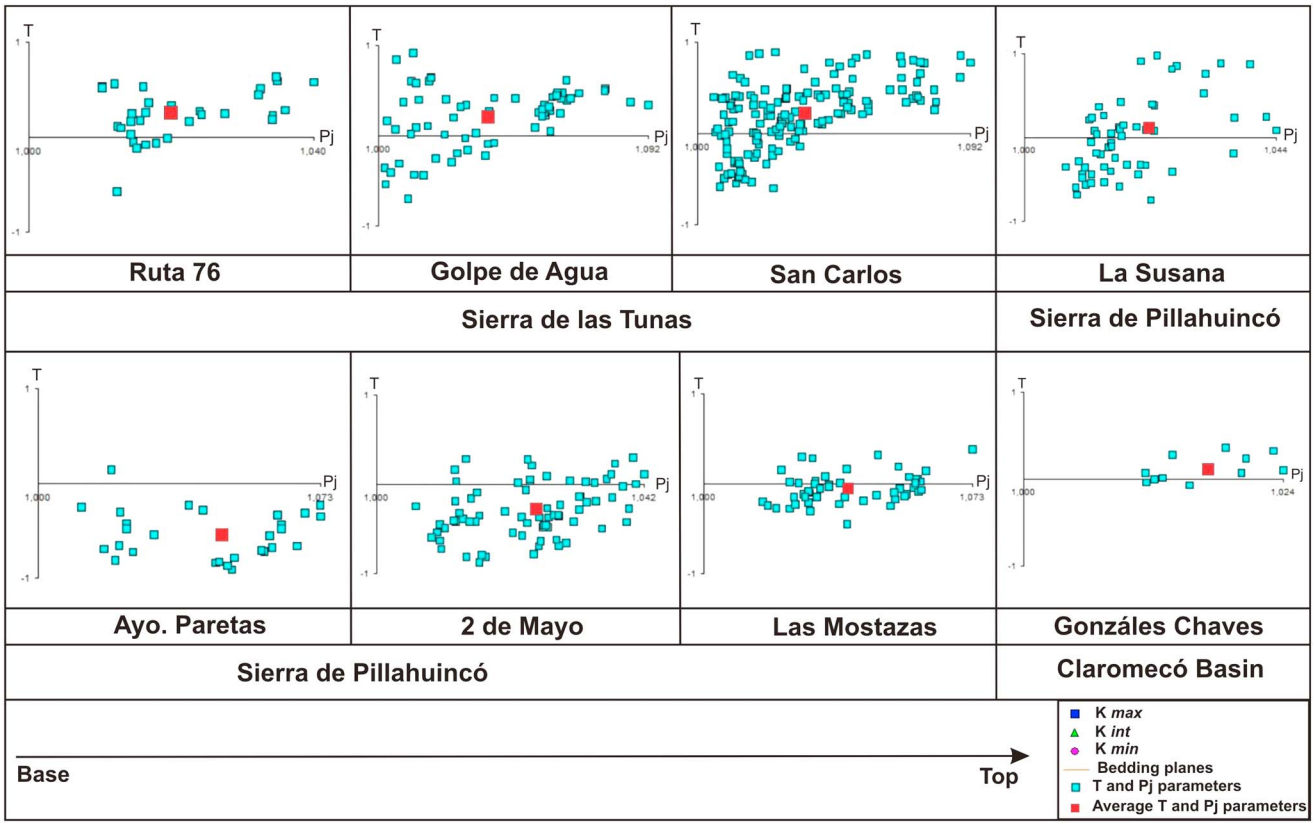

Figure 6. In the different localities, from base to top: Shape parameter (T) and degree of anisotropy (P_j), according to *Jelinek* [1981] parameters. The average of the T and P_j parameters is show in the red square for each locality. T values show mostly triaxial shapes of the ellipsoids, with different tendency to oblate (T average higher than 1, for example, in San Carlos locality) or prolate (T average lower than -1, for example, in 2 de Mayo locality).

localities, the K_{min} axes are almost horizontal, trending southwest-northeast, perpendicular, or scatter away from the bedding poles, show a transition to a tectonic fabric with a maximum compressive stress (σ_1) parallel to that direction (Figure 5). In contrast, toward the foreland, in the easternmost localities, at the top of the sedimentary column, the K_{min} axes orient vertically, showing a transition to a dominant sedimentary fabric (Figure 5).

In fact, the structural correction, done by restoring the beds to the horizontal plane through a single rotation around strike, shows no changes between the K_{max} orientation in situ or restored nor in the orientation of the K_{min}, to be more clustered in the restored position, which supports its syntectonic origin. However, it is clear on a regional scale that K_{min} changes from a subhorizontal position at the base of the unit (see Ruta 76) to a vertical one toward the foreland and top of the succession (Las Mostazas and Gonzáles Chaves; Figure 5).

The degree of anisotropy, P_j [*Jelinek*, 1981; *Tarling and Hrouda*, 1993], increases to maximum values up to 9% in some specimens in the localities situated at the base of the Tunas Formation, with average values between 1.7% and 4.7%, with the lower values at the Gonzáles Cháves locality (Table 2 and Figures 1 and 6). The standard deviation of P_j and T values are smaller than 0.025 and 0.048, respectively (Table 2 and Figure 7a). However, the values do not have a great variation and the errors overlap significantly (Figure 7a).

The shape parameter, T [*Jelinek*, 1981; *Tarling and Hrouda*, 1993], shows ellipsoids changing along the stratigraphic succession. Samples from localities at the base of the Sierra de las Tunas (Ruta 76, Golpe de Agua, and San Carlos), show oblate shapes ($T > 0$), with a K_{min} almost horizontal, while samples from localities at the Sierra de Pillahuincó show prolate ellipsoids ($T < 0$, in 2 de Mayo and Arroyo Paretas) or triaxial shapes ($T \approx 0$, in La Susana and Las Mostazas), with a K_{min} vertically oriented. In Gonzáles Chaves, where the strata are horizontal, the ellipsoids are predominantly oblate with K_{min} oriented vertically, indicating a transition to a sedimentary fabric (Figure 7).

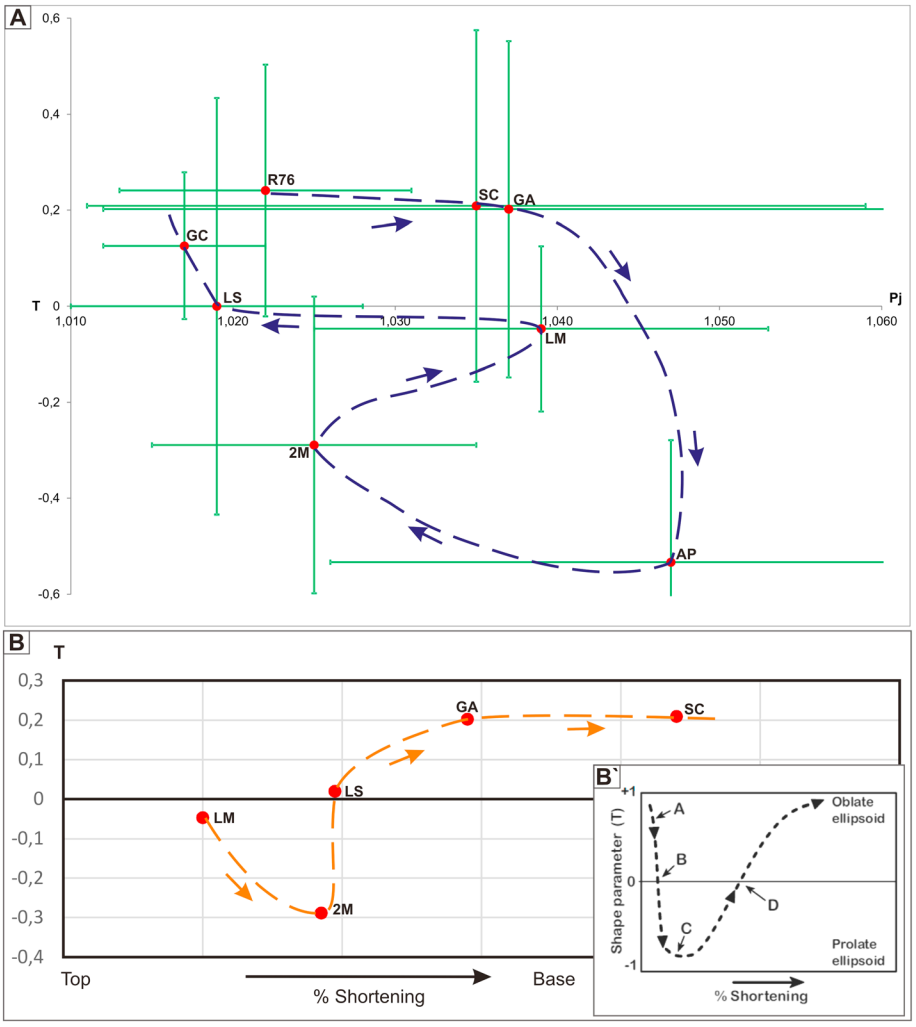

Figure 7. (a) Average anisotropy degree (P_j) related to the average shape parameter (T); the green lines are the standard deviation values of the P_j and T parameters (based on *Saint-Bezar et al*. [2002], *Parés and van der Pluijm* [2003], and *Weil and Yonkee* [2009]). These values are in Table 2. The blue arrows direction indicates the position of the localities along the stratigraphic succession, from the base to the top. (b) Evolution in the ellipsoids shape parameter according to the T values and the estimated shortening percent obtained by *Tomezzoli and Cristallini* [2004] in some localities. (b`) Comparison with conceptual models [*Saint-Bezar et al*., 2002; *Parés and van der Pluijm*, 2003; *Weil and Yonkee*, 2009]. The orange arrows indicate the increase of the shortening. R76: Ruta 76; LS: La Susana; SC: San Carlos; GA: Golpe de Agua; AP: Arroyo Paretas; LM: Las Mostazas; 2 M: 2 de Mayo; and GC: Gonzáles Chaves. There are changes in the shape of the ellipsoids, from triaxial to prolate and oblate indicating a migration from tectonic to sedimentary fabric.

6. Compaction Results

The compaction was estimated in medium-grained sandstones that belong to Facies 2 of the Tunas Formation, which is the coarsest and easier to estimate the contacts between the grains by applying the *Wilson and McBride* [1988] method.

At the base of the succession there is a predominance of sutured and concave-convex contacts, while toward the top there are predominantly straight and point contacts. The samples from Gonzáles Chaves have a predominance of point contacts (Table 3 and Figure 8). The TPI shows values of 0.78 in the localities located at the base and of 0.27 at the top of the Tunas Formation, in Gonzáles Chaves (Table 3 and Figure 8). This indicates more compaction at the base of the succession and less compaction values toward the top and in the easternmost localities. In general, all the values obtained are low, and they would indicate a burial depth below 1000 m [*McBride et al*., 1990].

Table 3. Count of the Different Types of Contacts (s: Sutured; c: Concave Convex; r: Straight; p: Punctual; f: Floating) and Total of Contacts and TPI Values Calculated According to *Wilson and McBride* [1988]

Sample	Locality	s	c	r	p	f	Total	TPI	TPI average
1140910	Ruta 76	378	357	857	386	65	2043	0.779	0.779
2050711	Ea La Susana	478	546	1150	422	81	2677	0.811	0.811
Y105	2 de Mayo	342	570	1262	486	110	2770	0.785	0.785
M9	Las Mostazas	238	68	780	1644	1846	4576	0.675	0.686
2030711b	Las Mostazas	187	333	1249	560	197	2526	0.2325	
4030711	Las Mostazas	542	616	1199	371	23	2751	0.856	
1070612[a]	Las Mostazas	204	215	775	320	50	1564	0.763	
01070612B	Las Mostazas	207	311	723	326	66	1633	0.761	
01070612C	Las Mostazas	345	317	718	264	17	1661	0.831	
CHCi	Gonzáles Chaves	54	58	370	1310	1999	3791	0.126	0.27
CHCi bis	Gonzáles Chaves	204	274	540	627	798	2443	0.417	

7. Interpretation and Integration of These Results in a Regional Context

Along and across the Tunas Formation there are evident changes in the AMS parameters, such as in the shape parameter (T) and in the K_{min} position toward the center of the basin.

The ratio between T and P_j and the ratio between T and the shortening values (calculated by *Tomezzoli and Cristallini* [2004], based on the structural cross section restauration) show both a pattern that changes with location in the stratigraphic succession and with shortening. In the western localities, at the base of the stratigraphic succession, with major tectonic deformation, the ellipsoids tend to have prolate-oblate shapes; toward the top, they tend to have triaxial and prolate shapes, and in the foreland basin, in the Claromecó Basin, with bed-parallel sedimentary fabric, the ellipsoids tend to have triaxial-oblate shapes (Figures 7a and 7b). This pattern is similar to the theoretical models of *Saint-Bezar et al.* [2002], *Parés and van der Pluijm* [2003], and *Weil and Yonkee* [2009], where weakly to strongly deformed sedimentary rocks in fold and thrust belts changed their AMS response. The AMS ellipsoids that have oblate shapes

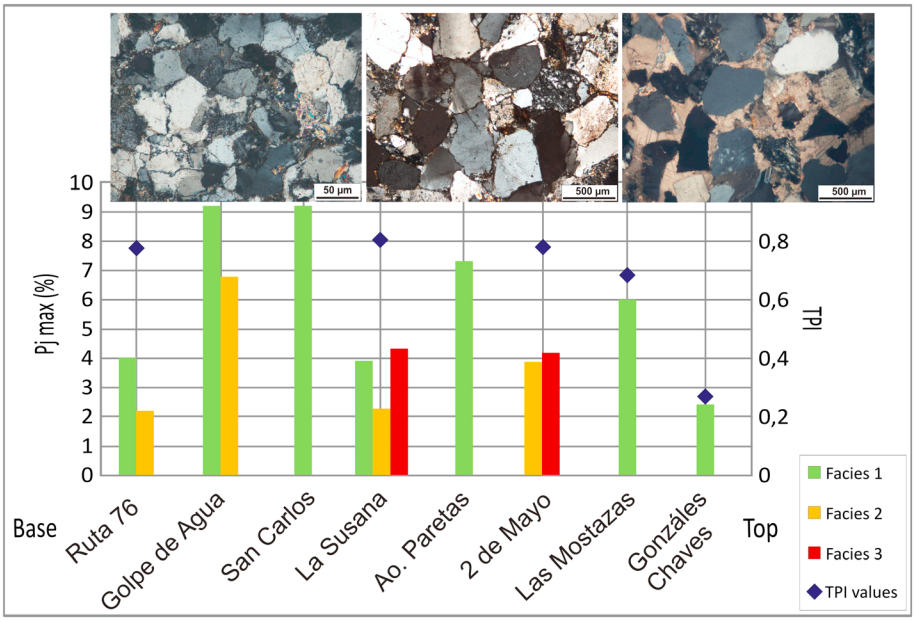

Figure 8. In the left vertical axis: maximum AMS degree (P_{jmax}) for each facies from different localities of the Tunas Formation. Facies 1 specimens show a clearer decrease of values to the top/foreland than the other facies, but we do not rule out the possibility that it could be an artifact of the decreasing sample numbers measured from Facies 1 to 2 and 3. In the right vertical exe: TPI values in each locality of the Tunas Formation. Above: Microphotograph showing a closer packing in the samples situated at the base than the samples sited at the top of the succession. The TPI values decrease toward the top of the Tunas Formation. See the correlation between the P_j and the TPI values.

Figure 9. Apparent polar wander path of Gondwana for the Late Paleozoic proposed by *Tomezzoli* [2009], with the paleomagnetic results of the Tunas Formation: Tunas I [*Tomezzoli and Vilas*, 1999] and Tunas II [*Tomezzoli*, 2001] PPs (red points) and other recently published paleomagnetic poles [*Tomezzoli et al.*, 2013]. The differences in the type and age of the magnetization between the lower and upper parts of the Tunas Formation, and therefore the two different paleomagnetic poles positions, are in accordance with the geological differences between the base and the top of the succession, the compaction degree and the AMS results described here, suggesting that the deformation was diachronous and propagated more slowly toward the foreland.

in the more tectonically deformed zones change to prolate-triaxial shapes and then to oblate shapes [*Saint-Bezar et al.*, 2002; *Parés and van der Pluijm*, 2003; *Weil and Yonkee*, 2009]. These changes indicate composite sedimentary/tectonic fabrics with layer parallel shortening (LPS) (Figure 7b). The lineation (K_{max}), which indicates the maximum elongation direction, is controlled by a secondary LPS [*Weil and Yonkee*, 2009].

In the Tunas Formation the K_{max} axes trend northwest-southeast, parallel to the fold axes, clusters parallel to the intersection of the LPS fabric with bedding, and tend to be constant in all sampled localities (Figure 5). The foliation (K_{min}) indicates that the shortening is related to the primary bedding. At the base of the sedimentary column, at the western most and also more deformed localities, the K_{min} axes are almost horizontal, trending southwest-northeast, perpendicular, or scatter away from the bedding poles, showing a transition to a tectonic fabric with a maximum compressive stress (σ_1) parallel to that direction (Figure 5), indicating moderate LPS. In contrast, toward the foreland, to the eastern most localities, to the top of the stratigraphic succession, the K_{min} axes tend to orient vertically, showing a transition to a sedimentary fabric and indicating minor LPS (Figure 5).

The localities to the base of the unit, with the highest values of shortening, show oblates to prolates ellipsoids indicating moderate lateral parallel shorting (LPS), with K_{min} parallel to the maximum shortening direction with composite tectonic to sedimentary/tectonic fabric, caused by overburden synchronously with the deformation during the deposition of the sediments [*Parés*, 2015; *Weil and Yonkee*, 2009] (stages D to C of *Weil and Yonkee* [2009] model; Figure 7). At the localities to the top of the unit, with minor values of shortening,

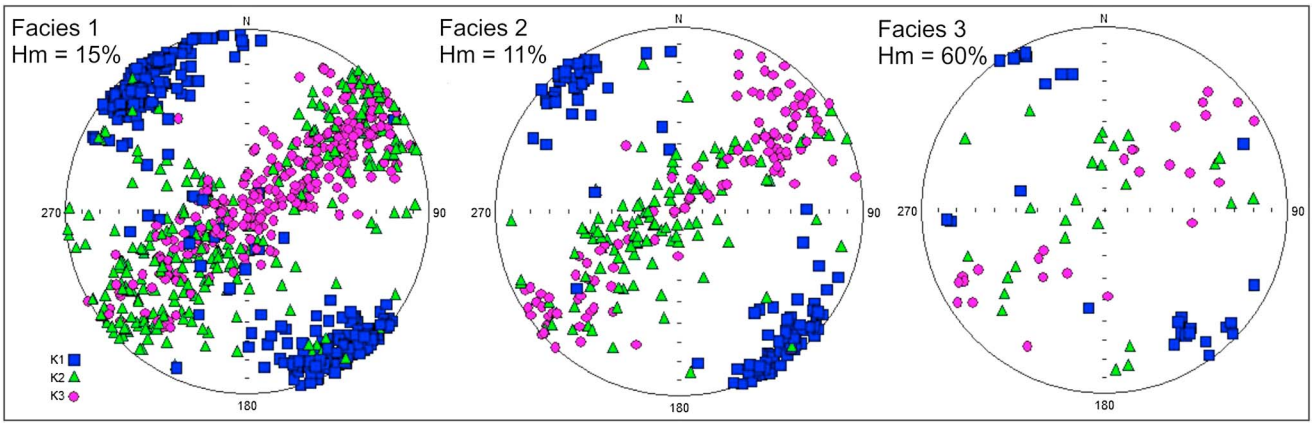

Figure 10. AMS data grouped by facies from all localities of the Tunas Formation in situ. The axes K_1 (K_{max}) remain in the same northwest-southeast direction and K_2 (K_{int}) and K_3 (K_{min}) remain as a vertical girdle, perpendicular to the fold axes, independently of the lithology. The three facies can be found either at the base or at the top of the succession.

the ellipsoids change progressively from prolate to triaxial. Finally, in Gonzáles Chaves, the ellipsoids tend to triaxial to oblate shapes again, resulting of a transition to a sedimentary fabric (Figure 7). This is consistent with the decrease of the deformation degree toward the eastern localities.

The differences in the AMS results among the localities at the Sierra de las Tunas (base) and Sierra de Pillahuincó (top) agree with:

1. Differences in the deformation style: different geometry of the folds that is clearly visible in the outcrops and in the shortening values (Figure 2).
2. Different types of magnetization. The characteristic remanent magnetization changes from the base to the top of the succession. While at the base it is clearly syntectonic, to the top of the succession the magnetization is less affected by the deformation. The main grouping of the characteristics remanent magnetization is reached at the base of the succession at 32% of unfolding while at the top of the succession is needed a 90% of unfolding to reach it. Based on this, two different paleomagnetic pole (PP) positions have been calculated: Tunas I and Tunas II PPs, respectively [*Tomezzoli and Vilas*, 1999; *Tomezzoli*, 2001] (Figure 9). The presence of syntectonic magnetizations with different percentages of unfolding demonstrates that the tectonic shortening diminishes toward the top. Thus, this pattern of sedimentation, folding and, magnetization indicates that the rocks were remagnetized during a relatively short period of time, as folding propagated more slowly toward the eastern foreland between the Early and Late Permian.
3. Different TPI values between the base and the top (Figure 8).

It is necessary to highlight that the orientations of the K_{max} axes remain constant in the geographic coordinates in all the localities (Figures 5 and 10).

Similar differences in the AMS patterns were obtained from nearby areas as the Carapacha Basin [*Tomezzoli et al*., 2006] (see location in the Figure 1) and the Sierra Chica site, belonging to the Choiyoi Magmatic Province [*Tomezzoli et al*., 2013] (see location in Figure 1), which are the same age as the Tunas Formation [*Melchor and Césari*, 1991, 1997]. As shown in Figure 11, these localities, based on the AMS and paleomagnetic results, also show clear tectonic features at the base of the succession, which are attenuated to the top.

According to *Tomezzoli* [1999, 2001, 2012], the deformation on the southwestern Gondwana continent margin began during the Late Devonian and is related to the collision of Chilenia from the west and Patagonia from the southwest [*Tomezzoli*, 2012]. These collisions occurred during the Cháñica orogenic phase [*Azcuy and Caminos*, 1987]. This deformation continued until the Late Paleozoic and is related to the postcollisional San Rafael or Gondwanic orogenic phase in the Late Carboniferous to Middle Permian [*Azcuy and Caminos*, 1987], as a movement to equatorial positions, which reorganized and adjusted all the plates previously accreted to Gondwana (southern plates) and Laurentia continents to finally form the Pangea supercontinent [*Wegener*, 1929] during the Triassic.

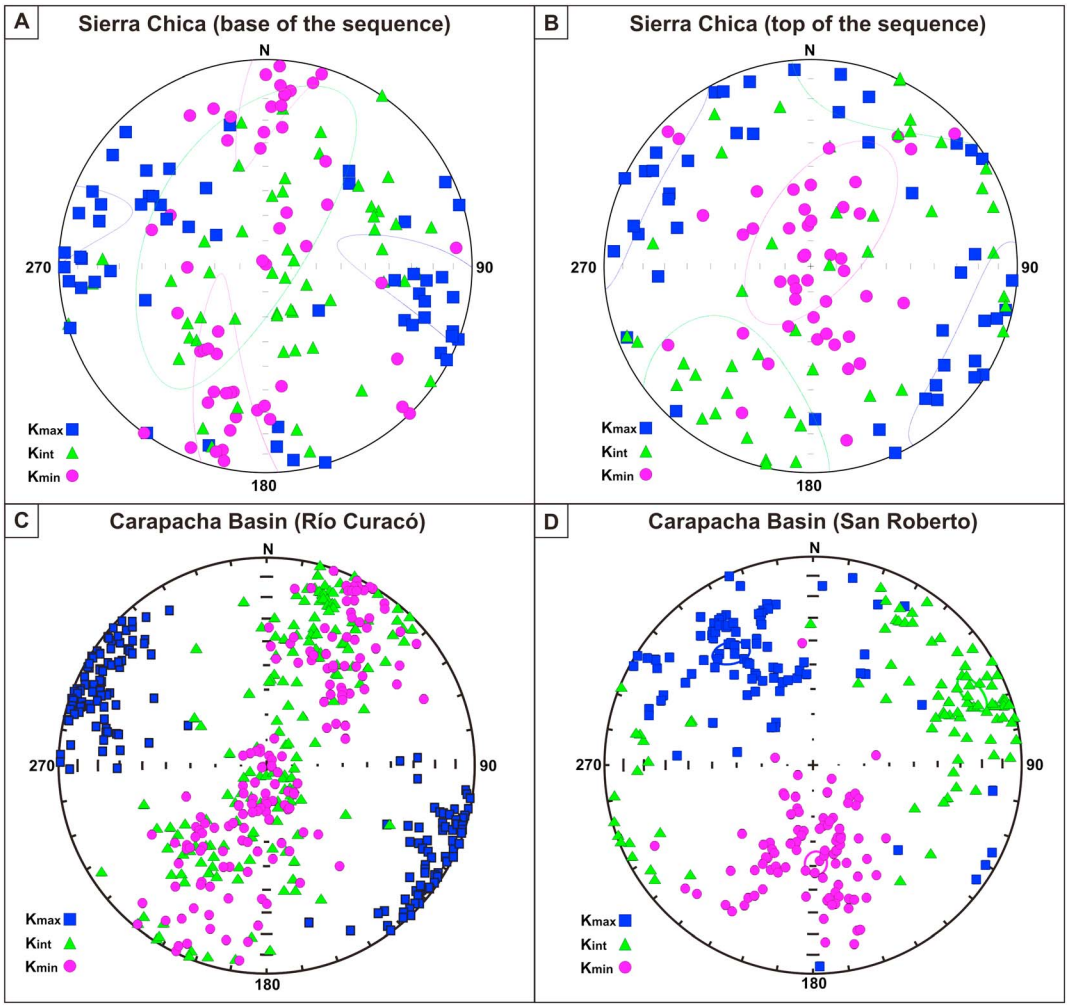

Figure 11. AMS mean directions from the Upper Paleozoic neighboring basin along the west Gondwanides belt: (a) and (b) Choiyoi magmatic Province [*Tomezzoli et al.*, 2013]; (c and d) Carapacha Basin, La Pampa Province [*Tomezzoli et al.*, 2006]. The AMS directions are similar all along the belt indicating a compression with a southwest direction.

8. Conclusions

The AMS data in the Tunas Formation (Sierras Australes-Claromecó Basin-southwest Gondwana boundary) show good internal consistency within the sites, the localities and among them. The data indicate that there is a syntectonic and syndepositional primary magnetization and petrofabric, carried dominantly by hematite.

The different facies, which are exposed throughout the entire column, show similar AMS patterns and directions as the principal ellipsoids axes. This implies that the lithology does not seem to have a relevant control over them. The observed changes in the AMS patterns and directions of the principal ellipsoids axes are controlled by the deformation, clearly by layer parallel shortening, which are synsedimentary, and varies according to the stratigraphic position. The differences between the base and the top of the succession are consistent with the stratigraphic position, the compaction degree, and the structural and paleomagnetic results already described here and studied in nearby regions along the southwest Gondwana margin. In all localities, the K_{max} axes are well grouped, situated to the northwest-southeast quadrant almost horizontal and parallel to the axes of the folds. However, at the base and in the older localities (with greater deformation, higher compaction levels and syntectonic magnetizations) the K_{min} axes tend to occupy horizontal positions, perpendicular to the fold axes, demonstrating the clear influence of the tectonic compression that developed a tectonic oblate to prolate fabric. On the other hand, as we move toward the top of the succession to younger localities, where the magnetizations are less affected by the tectonic compression, the K_{min} axes tend to move

to the vertical, demonstrating a change from tectonic to transitional prolate to triaxial or sedimentary oblate fabric due to compaction in the center of the basin (for example, in Gonzáles Chaves). The differences are clearly defined between the opposite localities of the sedimentary column: Ruta 76 (base) and Gonzáles Chaves (top). The magnitude of the anisotropy also gradually decreases toward the foreland basin.

All the results combine different methodologies that indicate that the deformation along the Gondwana margin propagated from the southwest, gradually diminished during the Early to Late Permian, evidencing an orogenic front migration to the foreland basin toward the northeast. This noncollisional deformation is due to the final movements toward the Equator and rearrangement of the Gondwanic and Laurentian tectonic plates that produce a change in their orientation, relative to the geographical South and North Poles, respectively, with latitudinal and small counterclockwise/clockwise movements during the Permian to form the Triassic Pangea.

Acknowledgments
We thank the Laboratorio de Paleomagnetismo "D.A. Valencio" at the FCEyN, Universidad de Buenos Aires (UBA), and the Departamento de Geología of Universidad Nacional del Sur in Bahía Blanca, for providing the equipment necessary to carry out the measurements of the specimens. The Technology Vinculation Projects "Ingeniero Enrique Mosconi," PIP-CONICET 099, for the funding that enabled the conduction of these studies, and the Comisión de Investigaciones Científicas (CIC) for the Doctoral Grant. Our thanks also go to Ernesto O. Cristallini, Leandro C. Gallo, and Augusto E. Rapalini for their collaboration during the preparation of this work and especially to Gustavo Tolson and an anonymous reviewer whose comments helped us to considerably improve this work. Supporting data are included as three tables and eleven figures; any additional data may be obtained from the main authors (e-mails: guadalupe.arzadun@gmail.com and rtomezzoli@gmail.com). Also additional structural data may be obtained from Ernesto Cristallini (e-mail: ecristallini@gmail.com).

References

Álvarez, G. T. (2004), Cuencas Paleozoicas asociadas a la prolongación norte del sistema de Sierras de Ventania, Provincia de Buenos Aires, PhD thesis, Universidad Nacional del Sur, Argentina, 184 pp.

Amos, A. J., and C. M. Urien (1968), La falla "Abra de la Ventana" en las Sierras Australes de la provincia de Buenos Aires, *Rev. Asoc. Geol. Argent.*, *23*(3), 197–206.

Andreis, R. R., and G. Cladera (1992), Las epiclastitas pérmicas de la Cuenca Sauce Grande (Sierras Australes, Buenos Aires, Argentina). Parte 1: Composición y procedencia de los detritos, Actas 4° Reunión de Sedimentología. La Plata. 1, 127-134.

Andreis, R. R., J. J. Lluch, and A. M. Iñiguez Rodríguez (1979), Paleocorrientes y paleoambientes de las Formaciones Bonete y Tunas, Sierras Australes de la Provincia de Buenos Aires, Argentina, Actas 6° Congreso Geológico Argentino, Buenos Aires. 2: 207-224.

Andreis, R. R., A. M. Iñiguez Rodríguez, J. J. Lluch, and S. Rodríguez (1989), Cuenca paleozoica de Ventania. Sierras Australes de la provincia de Buenos Aires, in *Cuencas sedimentarias argentinas*, *Serie Correlación Geológica*, vol. 6, edited by G. Chebli and L. Spalletti, pp. 265–298, San Miguel de Tucumán, Argentina.

Archangelsky, S., and R. Cúneo (1984), Zonación del Pérmico continental de Argentina sobre la base de sus plantas fósiles, 3° Congreso Latinoamericano Paleontológico, México. Memory, pp. 143-153.

Arzadún, G. (2015), Análisis del soterramiento de la Formación Tunas en las Sierras Australes de la Provincia de Buenos Aires a partir de índices de compactación y de empaquetamiento, PhD thesis, Universidad Nacional del Sur, 243 p.

Arzadún, G., J. I. Falco, N. N. Cesaretti, and R. N. Tomezzoli (2014), Nódulos y concreciones de hematita en la Formación Tunas (Pérmico de Sierras Australes, Provincia de Buenos Aires): Su potencialidad como indicadores diagenéticos y ambientales. Proceedings of XVI Reunión Argentina de Sedimentología, pp. 31–32.

Azcuy, C. L., and R. Caminos (1987), in *Diastrofismo en El Sistema Carbonífero en la República Argentina*, edited by S. Archangelsky, pp. 239–251, Academia Nacional de Ciencias, Córdoba.

Borradaile, G. J. (1988), Magnetic susceptibility, petrofrabrics and strain, *Tectonophysics*, *156*, 1–20.

Bowen, B. B., K. C. Benison, F. E. Oboh-Ikuenobe, S. Story, and M. R. Mormile (2008), Active hematite concretion formation in modern acid saline lake sediments, Lake Brown, Western Australia, *Earth Planet. Sci. Lett.*, *268*(1-2), 52–63.

Buggisch, W. E. (1987), Stratigraphy and very low grade metamorphism of the Sierras Australes de la Provincia de Buenos Aires (Argentina) and implications in Gondwana correlation, *Zbl. Geol. Paläontol. Teil I*, *7/8*, 819–837, Stuttgart.

Chernicoff, C. J., E. O. Zappettini, J. O. S. Santos, E. Belousova, and N. J. McNaughton (2013), Combined U-Pb SHRIMP and Hf isotope study of the Late Paleozoic Yaminué Complex, Río Negro province, Argentina. Implications for the origin and evolution of the Patagonia composite terrane, *Geosci. Front.*, *4*(6), 37–56.

Cobbold, P., D. Gapais, and E. Rossello (1991), Partitioning of transpressive motions within a sigmoidal foldbelt: The Variscan Sierras Australes, Argentina, *J. Struct. Geol.*, *13*, 743–758.

Cobbold, P. R., A. C. Massabie, and E. A. Rossello (1987), Hercynian wrenching and thrusting in the Sierras Australes Foldbelt, Argentina, *Hercynica*, *2*(2), 135–148.

Du Toit, A. L. (1927), A geological comparison of South America with South Africa, *Carnegie Inst. Wash. Publ.*, *381*, 1–157.

Flinn, D. (1962), On folding during three-dimensional progressive deformation, *Q. J. Geol. Soc. London*, *118*, 385–433.

Graham, J. W. (1954), Magnetic susceptibility, an unexploited element of petrofabric, *Geol. Soc. Am. Bull.*, *65*, 1257–1258.

Gregori, D. A., L. E. Grecco, and E. J. Llambías (2003), El intrusivo López Lecube: Evidencias de magmatismo alcalino Gondwánico en el sector sudoeste de la provincia de Buenos Aires, Argentina, *Rev. Asoc. Geol. Argent.*, *58*(2), 167–175.

Gregori, D. A., J. Kostadinoff, L. Strazzere, and A. Raniolo (2008), Tectonic significance and consequences of the Gondwanide orogeny in northern Patagonia, Argentina, *Gondwana Res.*, *14*, 429–450, Elsevier.

Harrington, H. J. (1947), Explicación de las Hojas Geológicas 33 m y 34 m, Sierras de Curamalal y de la Ventana, Provincia de Buenos Aires. Servicio Nacional de Minería y Geología, *Boletín*, *61*, 43.

Iñiguez, A. M., and R. R. Andreis (1971), Caracteres sedimentológicos de la Formación Bonete, Sierras Australes de la provincia de Buenos Aires. Reunión Geológica de las Sierras Australes Bonaerenses. Provincia de Buenos Aires. Comisión de Investigaciones Científicas. La Plata, pp. 103–120.

Iñiguez, A. M., R. R. Andreis, and P. A. Zalba (1988), Eventos piroclásticos en la Formación Tunas (Pérmico), Sierras Australes, Provincia de Buenos Aires. Actas II, Jornadas Geológicas Bonaerenses, 383–395.

Jackson, M. J. (1991), Anisotropy of magnetic remanence: A brief review of mineralogical sources, physical origins, and geological applications, and comparison with susceptibility anisotropy, *Pure Appl. Geophys.*, *136*, 1–28.

Japas, M. S. (1995a), Evolución estructural de la porción austral del arco de las Sierras Australes de Buenos Aires, *Rev. Asoc. Geol. Argent.*, *49*(3), 368–372.

Japas, M. S. (1995b), El Arco Noroccidental de las Sierras Australes de Buenos Aires: Producto de mega kinks extensionales durante el proceso de la deformación?, Actas 4° Jornadas Geológicas Bonaerenses, 1: 257-263. Junín.

Japas, M. S. (1999), Revisión de las teorías acerca del origen del arco de las Sierras Australes de Buenos Aires, *Rev. Asoc. Geol. Argent.*, *54*(1), 9–22.

Jelinek, V. (1981), Characterization of the magnetic fabrics of Rocks, *Tectonophysics*, *79*, 63–67.

Keidel, J. (1916), La geología de las Sierras de la provincia de Buenos Aires y sus relaciones con las montañas del Cabo y los Andes, Min. Agric. Nac., An. Dir. Nac. Geol. Min., IX, 3. Buenos Aires. 9: 5-57.
Kilmurray, J. O. (1975), Las Sierras Australes de la Provincia de Buenos Aires, las facies de deformación y nueva interpretación estratigráfica, *Rev. Asoc. Geol. Argent.*, *30*(4), 331–348.
Kostadinoff, J. (1993), Geophysical evidence of a Paleozoic Basin in the interhilly area of Buenos Aires Province, Argentina, Comptes Rendus XII ICCP. Volumen 1: 397-404.
Kostadinoff, J. (2007), Evidencia geofísica del umbral de Trenque Lauquen en la extensión norte de la Cuenca de Claromecó, Provincia de Buenos Aires, *Rev. Asoc. Geol. Argent.*, *62*(1), 69–75.
Kostadinoff, J., and G. Font de Affolter (1982), Cuenca Interserrana Bonaerense, Argentina, 5° Congreso Latinoamericano de Geología, Actas 4: 105-121, Buenos Aires.
Kostadinoff, J., and C. Prozzi (1998), Cuenca de Claromecó, *Rev. Asoc. Geol. Argent.*, *53*(4), 461–468.
Lesta, P., and C. Sylwan (2005), Cuenca de Claromecó. VI Congreso de Exploración y Desarrollo de Hidrocarburos. Simposio Frontera Exploratoria de la Argentina, Eds: Chebli, G.A., J.S. Cortiñas, L.A. Spalletti, L. Legarreta and E.L. Vallejo, pp. 217–231.
Llambías, E. J., and C. R. Prozzi (1975), Ventania, 6° Congreso Geológico Argentino. Relatorio 79-102. Buenos Aires.
López Gamundi, O. R., P. J. Conaghan, E. A. Rossello, and P. R. Cobbold (1995), The Tunas Formation (Permian) in the Sierras Australes Foldbelt, east central Argentina: Evidence for syntectonic sedimentation in a foreland basin, *J. S. Am. Earth Sci.*, *8*(2), 129–142.
López Gamundi, O. R., A. Fildani, A. Weislogel, and E. Rossello (2013), The age of the Tunas Formation in the Sauce Grande basin-Ventana foldbelt (Argentina): Implications for the Permian evolution of the southwestern margin of Gondwana, *J. South Am. Earth Sci.*, *45*, 250–258.
McBride, E. F., T. N. Diggs, and J. C. Wilson (1990), Compaction of Wilcox and Carrizo Sandstones (Paleocene-Eocene) to 4420 m, Texas Gulf Coast, *J. Sediment. Petrol.*, *61*(1), 73–85.
Melchor, R. N., and S. N. Césari (1991), Algunos elementos paleoflorísticos de la Formación Carapacha (Pérmico inferior), provincia de La Pampa, República Argentina, *Ameghiniana*, *28*, 347–352.
Melchor, R. N., and S. N. Césari (1997), Permian floras from Carapacha Basin, La Pampa Province, central Argentina. Description and importance, *Geobios*, *30*(5), 607–633.
Monteverde, A. (1937), Nuevo yacimiento de material pétreo en González Chaves, *Rev. Mineral.*, *8*, 116–124.
Nagata, T. (1961), *Rock Magnetism*, 2nd ed., pp. 350, Maruzen, Tokyo.
Pángaro, F., and V. A. Ramos (2012), Paleozoic crustal blocks of onshore and offshore central Argentina: New pieces of the southwestern Gondwana collage and their role in the accretion of Patagonia and the evolution of Mesozoic south Atlantic sedimentary basins, *Mar. Pet. Geol.*, *37*(1), 162–183.
Pángaro, F., V. A. Ramos, and P. J. Pazos (2015), The Hesperides basin: A continental-scale upper Palaeozoic to Triassic basin in southern Gondwana, *Basin Res.*, *1-27*.
Parés, J. M. (2015), Sixty years of anisotropy of magnetic susceptibility in deformed sedimentary rocks, *Front Earth Sci.*, *3*, 1–13.
Parés, J. M., and B. A. van der Pluijm (2003), Magnetic fabrics and strain in pencil structures of the Knobs Formation, Valley and Ridge Province, US Appalachians, *J. Struct. Geol.*, *25*, 1349–1358.
Ramos, V. A. (1984), Patagonia: Un nuevo continente paleozoico a la deriva?, 9° Congreso Geológico Argentino (S. C. Bariloche). Actas. 2: 311-325.
Ramos, V. A., F. Chemale, M. Naipauer, and P. J. Pazos (2013), A provenance study of the Paleozoic Ventania System (Argentina): Transient complex sources from Western and Eastern Gondwana, *Gondwana Res.*, *26*, 719–740.
Rossello, E. A., and A. C. Massabie (1981), Micro y mesoestructuras en las formaciones Lolén y Sauce Grande y sus implicancias tectónicas. Sierras Australes de Buenos Aires, *Rev. Asoc. Geol. Argent.*, *36*(3), 272–285.
Rossello, E. A., and A. C. Massabie (1992), Caracterización tectónica del kinking mesoscópico de las Sierras Australes de Buenos Aires, *Rev. Asoc. Geol. Argent.*, *47*(2), 179–187.
Saint-Bezar, B., R. L. Herbert, C. Aubourg, P. Robion, R. Swennen, and D. Frizon de Lamotte (2002), Magnetic fabric and petrographic investigation of Hematite bearing sandstones within ramp-related folds: Examples from the South Atlas Front (Morocco), *J. Struct. Geol.*, *24*, 1507–1520.
Suero, T. (1972), Compilación geológica de las Sierras Australes de la provincia de Buenos Aires, Ministerio de Obras Públicas, LEMIT, División Geología. Anales 3: 135-147. La Plata.
Tarling, D. H., and F. Hrouda (1993), *The Magnetic Anisotropy of Rocks*, pp. 217, Chapman and Hall, London.
Taylor, J. M. (1950), Pore-space reduction in sandstones, *Am. Assoc. Pet. Geol. Bull.*, *34*(4), 701–716.
Tomezzoli, R. N. (1997), Geología y Paleomagnetismo en el ámbito de las Sierras Australes de la provincia de Buenos Aires, PhD thesis, Universidad de Buenos Aires, 306 p.
Tomezzoli, R. N. (1999), La Formación Tunas en las Sierras Australes de la Provincia de Buenos Aires. Relaciones entre sedimentación y deformación a través de su estudio paleomagnético, *Rev. Asoc. Geol. Argent.*, *54*(3), 220–228.
Tomezzoli, R. N. (2001), Further palaeomagnetic results from the Sierras Australes fold and thrust belt, Argentina, *Geophys. J. Int.*, *147*, 356–366.
Tomezzoli, R. N. (2009), The apparent polar wander path for South America during the Permian-Triassic, *Gondwana Res.*, *15*, 209–215.
Tomezzoli, R. N. (2012), Chilenia y Patagonia: Un mismo continente a la deriva?, *Rev. Asoc. Geol. Argent.*, *69*(2), 222–239.
Tomezzoli, R. N., and E. O. Cristallini (1998), Nuevas evidencias sobre la importancia del fallamiento en la estructura de las Sierras Australes de la Provincia de Buenos Aires, *Rev. Asoc. Geol. Argent.*, *53*(1), 117–129.
Tomezzoli, R. N., and E. O. Cristallini (2004), Secciones estructurales de las Sierras Australes de la provincia de Buenos Aires: Repetición de la secuencia estratigráfica a partir de fallas inversas?, *Rev. Asoc. Geol. Argent.*, *59*(2), 330–340.
Tomezzoli, R. N., and J. F. Vilas (1999), Paleomagnetic constraints on age of deformation of the Sierras Australes thrust and fold belt, Argentina, *Geophys. J. Int.*, *138*, 857–870.
Tomezzoli, R. N., R. Melchor, and W. D. McDonald (2006), Tectonic implications of post-folding Permian magnetizations, Carapacha basin, Argentina Paleomagnetism in Latinoamerica, Special Volume, *Earth Planets Space*, *58*, 1235–1246.
Tomezzoli, R. N., H. Vizán, H. Tickyj, and M. E. Woroszylo (2013), Revisión de la posición del polo paleomagnético de Sierra Chica, La Pampa, Argentina, en la curva de desplazamiento polar aparente del Gondwana Sudoccidental, *Latinmag Lett.*, *3*(3), 1–8.
Von Gosen, W., W. Buggisch, and S. Krumm (1989), Metamorphism and deformation mechanisms in the Sierras Australes fold and thrust belt (Buenos Aires Province, Argentina), *Tectonophysics*, *185*, 335–356.
Von Gosen, W., W. Buggisch, and L. V. Dimieri (1990), Structural and metamorphic evolution of the Sierras Australes (Buenos Aires Province/Argentina), *Geol. Rundsch.*, *79*(3), 797–821.
Von Gosen, W., W. Buggisch, and S. Krumm (1991), Metamorphism and deformation mechanisms in the Sierras Australes fold and thrust belt (Buenos Aires Province, Argentina), *Tectonophysics*, *185*, 335–356.
Walker, R. G., and N. P. James (1992), *Facies Models: Response to Sea Level Change*, pp. 409, Geological Association of Canada, Department of Earth Sciences, Memorial Univ. of Newfoundland, Canada.

Wegener, A. (1929), *Die Entstehung der Kontinente und Ozeane*, pp. 221, Friedrich Vieweg & Sohn Akt. Ges, Braunschweig.
Weil, A. B., and A. Yonkee (2009), Anisotropy of magnetic susceptibility in weakly deformed red beds from the Wyoming salient, Sevier thrust belt: Relations to layer-parallel shortening and orogenic curvature, *Lithosphere*, *1*(4), 235–256.
Wilson, J. C., and E. F. McBride (1988), Compaction and porosity evolution of Pliocene sandstones, Ventura basin, California, *AAPG Bull.*, *72*, 664–681.
Yoshida, H. D., K. Yamamoto, Y. Murakami, and K. Matsuoka (2006), Formation of biogenic iron-oxide nodules in reducing sediments as an analogue of near-field redox reaction products, *Phys. Chem. Earth*, *31*, 593–599.
Zambrano, J. J. (1974), Cuencas sedimentarias en el subsuelo de la provincia de Buenos Aires y zonas adyacentes, *Rev. Asoc. Geol. Argent.*, *29*, 443–469.
Zavala, C. A., M. F. Santiago, and G. E. Amaolo (1993), Depósitos fluviales de la Formación Tunas (Pérmico). Cuenca Paleozoica de Ventania, Provincia de Buenos Aires, *Rev. Asoc. Geol. Argent.*, *48*(3-4), 307–316.